INTERNATIONAL SOCIETY FOR SOIL MECHANICS AND GEOTECHNICAL ENGINEERING



This paper was downloaded from the Online Library of the International Society for Soil Mechanics and Geotechnical Engineering (ISSMGE). The library is available here:

https://www.issmge.org/publications/online-library

This is an open-access database that archives thousands of papers published under the Auspices of the ISSMGE and maintained by the Innovation and Development Committee of ISSMGE.

DEFORMATION AND STRENGTH OF SOILS

LA DEFORMATION ET LA RESISTANCE DES SOLS

ДЕФОРМИРУЕМОСТЬ И НРОЧИОСТЬ ГРУНТОВ

M. GOLDSTEIN, Prof., S. BABITSKAYA, M. Sc., Institute of Roilway Transport, Dniepropetrovsk G. LOMIZE, Prof., A. KRYZHANOVSKY, M. Sc., Civil Engineering Institute, Moscow, USSR

SYNOPSIS. In the part written by M.Goldstein and S.Babitskaya the method of accelerating the compression test in 5-7 times is described. It guarantees the accuracy not less than in standard tests. It is suggested to use the empirical relation between shear strength and effective normal octahedral stress for shear strength estimation under different conditions of testing.

In the second part (by G.Lomize) the influence of time factor on soil clay strain and strength is examined. These tests allowed to establish the regularities of time influence on the dilatation of the medium with the interaction of the stress development and on the deformation under different stress trajectories.

In the third part written by A.Kryzhanovsky the investigation of the pure shear of sands are described. It is shown that only special trajectories of stress development are realized under given type of strain. They represent the combination of unloading and loading and result in strain characteristics which differs from the test characteristics obtained under the other trajectories. The active role of the phase interaction in strain properties of skeleton in given physical state is shown.

I.A lot of consolidation tests under standard sample dimensions have shown that this process is well described by the empirical formula (fig.1a):

$$e_t = e_f + Ct^{-m} \tag{1}$$

where e, - the void ratio after the consolidation under given increment of the load;
t - the time elapsed after the putting given load increment;

C - the difference between the void ratio for t = 1 hour and the final e, value: m - a parameter, equal to 0,5 for disturbed clay sample.

The consolidation graph $e_t \sim t^{-0.5}$ for the disturbed clay sample ($w_L = 42.9\%$; $w_p = 24.6\%$; $I_p = 38.3\%$; $\chi_d = 1.33$ g/cm³, e = 1.03; $s_{\chi} = 1.03$; $s_{\chi} = 1.03$; so plotted in fig.1b. It consist of the two straights with inflection-point at $t_0 \approx 0.33$ hour. The dependence (1) can be considered as correct for practical use only from the moment t_0 (origin time) corresponding to this inflection-point. A physical cause of this inflection-point appeareance in all clay soils is not still clear enough. The value t_0 depends on the type of soil, but it don't exceed 1 hour in all cases.

The equation (1) was confirmed for the pres-

sures from 0,25 to 5,0 kg/cm² and for the great interval of plasticity index ($I_P = 8-40$). The samples were of different dry density, moisture content and structure.

Compression test can be accelerated by using equation (1) if each next load increment is applied without the soil stabilization under the prior one. Each load increment must act not less than 3-4 hours. Although the deformation under each load increment is in this method only 50-80% of its full value, the calculated void ratio coincide practically with all the test values as it can be seen from table 1 (for the above mentioned soil, fig.1).

The comparison of the teste and calculated values of void ratio.

Time in hours		Void r	Relative error	
1		2	3	4
0,12 0,17 0,33 0,5	2,94 2,44 1,72 1,41	0,913 0,910 0,902 0,895 0,887	0,934 0,922 0,903 0,895 0,884	2,3 1,3 0,1 0

1	2	3	4
2 0,71 3 0,58 4 0,50 5 0,45 8 0,35 19 0,23 29 0,18 43 0,15	0,878 0,875 0,873 0,871 0,868 0,865 0,863 0,861	0,876 0,873 0,871 0,870 0,867 0,864 0,863 0,862	0,2 0,2 0,2 0,1 0,1 0,1 0,1
93 0.11	0.859	0,861	0.2

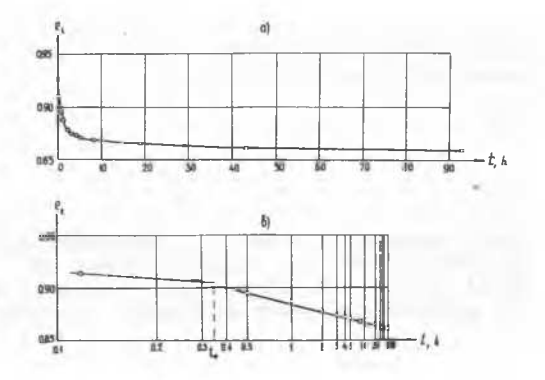


Fig.1. Relation between time and void ratio, $6 = 1.0 \text{ kg/cm}^2$.

a)e_t = f(t); b) e_t = f $(\frac{1}{\sqrt{t}})$

It is advisable to use two values e_t at any time from t_0 to t=3 or 4 hours for the parameters C and $e_{\frac{1}{2}}$ calculation.

The comparative values for wold ratio, coefficient of compressibility and modulus of deformation for the same clay, but with w=28,7%, $\chi_d=1,55$ g/cm³, e=0,740, $S_{\bar{b}}=1$ are shown in table 2.

Table 2
The comparison of the ordinary and accelerated compression test results

6 kg cm ²	Void :	9 _t	Coeffi of cor sibili cm ² /l	cient mpres- ity m _y Acce- lerat- ed me-	Modulu deform B. kg/ Ordi- nary	s of mation,
0	0,740	0,740				
0,25	0,720	0,723	•	0,092	12,5	10, 9
0.50	0,708	0,711	-	0,048	20,8	20,8
	0,688	-	0,040	0,044	25,0	22,8
-	0,652	-	0,035	0,038	27,8	26,3
	0.627		0,025	0,029	40,0	34,5

It can be seen that deformation characteristics determined by accelerated method (all the test is lasting only 2 days) are practically equal to the determined by ordinary method (the test is lasting 12-15 days).

The duration of accelerated and ordinary tests with loam were for 2 and 8 days accordingly and with montmorillonite clay were for 3 and 15-20 days accordingly.

The comparison of two methods is shown in fig.2. Maximum divergence δ does not exceed 0,075.

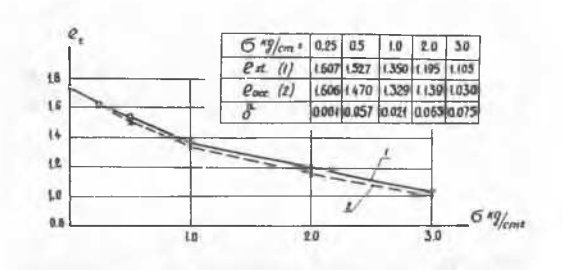


Fig.2. The comparison of the standard (1) and accelerated (2) compression tests; montmorillonite, w = w₁ = 58,6%.

Thus the suggested method allows to obtain within a short period of time the deformation characteristics suitable for practical purposes.

There are now no methods to determine the shear strength characteristics for the some test conditions using data obtained under another ones (different drain conditions, stress history etc). But this problem can be solved on the base of Terzaghi's well known principle of effective stresses.

In fig.3 the relation $\overline{G}_o \sim T_o$ obtained by the statistical handling of the triaxial compression tests of 100 different soil samples from different area (plasticity index varied from 8 to 18) is shown ($\overline{G}_o = \frac{G_1}{3} + \frac{G_2}{3} + \frac{G_3}{3} - u$; $C_s - failure tangential stress on octahedral plane; <math>u - pore pressure$).

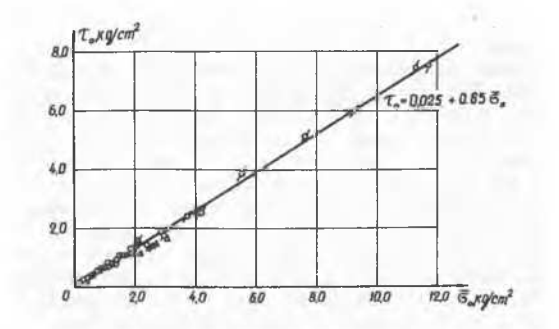


Fig. 3. Relation between shear strength and average effective spress $\hat{\nabla}_{o}$:

o -soil I (41 tests); x - soil II
(26 tests); a - soil III (15 tests);
ø - soil ¶Y (14 tests).

The samples with different initial physical state, overconsolidated or underconsolidated and with disturbed or undisturbed structure were sheared by the UU, UC and DC methods and under the following regimes of principal stress changing: a) $G_{\overline{n}} = \text{const}$; $G_{\overline{1}} - \text{increased}$; b) $\leq G = \text{const}$ ($G_{\overline{1}} - \text{increased}$).

The test results were so close that it was possible to unite them when statistical handling. The following expression was obtained for given soil type (= 8-18) by the least square method:

$$T_o = A + B G_o = 0.025 + 0.65 G_o$$
 (2)

It can be concluded that parameter A reflects the influence of the structure cohesion. For the clays of low sensitivity tested by KD-shear method parameter A must be nearly zero. That was confirmed by tests (A = 0,025). The correlation coefficient was equal to 0,997. The same tests give the great scattering if the pore pressure doesn't be taken into account, as it can be seen in fig.4.

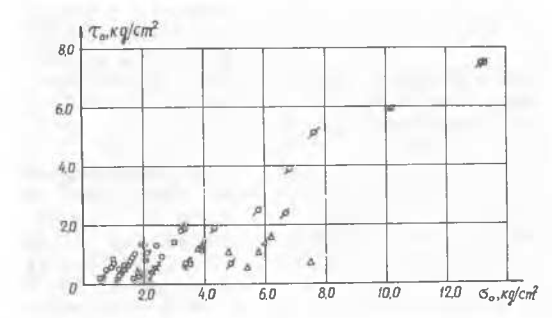


Fig.4. Relation between shear strength and average total stress ⊙ (without taking into account the pore pressure).

The above mentioned factors influence somehow the parameters of the equation (2), but making little noice in comparing with contribution made by the effective stresses.

Thus the dependence between shear strength and average effective stress is single-valued and has the same parameters for given type of clay soil and for any test condition. Practically there is no influence of apparatus type and test conditions on the test results. It means that tests may be carried out by using any known methods, but pore pressure must be measured in all cases to express the test results in terms of the effective stresses.

If in a laboratory the similar dependence with known parameters A and B was priory obtained then one can at once determine the designed shear strength for any other clay which belong to the same interval of plasticity index.

For transistion to another test condition it is necessary to determine only pore pressure u for principal stresses which corresponds to nature stress condition and initial physical state (dry density and water content).

The average effective stress is equal to

$$\bar{6}_{6} = \frac{6\bar{r}_{1} + 6\bar{r}_{1} + 6\bar{r}_{1}}{3} - u \qquad (3)$$

The shear strength is found by using (2) without special shear tests.

If the given soil was'nt tested before then it is necessary to carry out a triaxial test with 3-4 samples by using KU-shear method for plotting the dependence (2).

If a test with the pore pressure measuring can not be carried out by some cause then KD-shear method must be used as the main task of the recomended method is the determining the dependence between $\mathbb T$ and $\overline S_o$ under effective stress condition of soil.

II. This section of the Report was written by G.M.Lomize with the co-author A.A.Muza-farov. The experiments were conducted with compact clays of the upper Permian deposits of natural structure (soil No.1) and with disturbed loams (soil No.2). Composition and initial state of the soils are given in Table 3.

Table 3

Physical characteris- Grain size distributics						
Physical characte- ristics	Clay of na- tural struc- ture	Dis- turb- ed	Fraction diameter	- So: Clay of na- tural struc- ture	Dis- turb- ed	
1. (g/cm ³)	1.81	1.72	0.5-0.25	_	0.7	
2,₩ (%)	19.2	18.3	0,25-0.1	0.74	4.0	
3 , e	0.54	0.58	0.1-0.05	37.76	14.7	
4.Sx	0.97	0.85	0.05-0,01	14.6	35.4	
5						
\(\(\(\text{g/cm}^{\dagger} \)	2.77	2.72	0.01-0.005	3 •7	19,2	
6.W _{T.} (%)	44.7	30	0.005-0.001	19.5	19.2	
$7.W_{D}(\%)$	19.5	20	<0.001	23.7	6.8	
	25.2	10				

The experiments were conducted under threedimensional stress condition on a triaxial apparatus as well as on arrangements I and II designed in the Moscow Institute of Civil Engineers [1,2]. These arrangements allow the control of the three principal stresses (arrangements I and II) and rotation of the axes of the principal stress (the arrangement I). Experiments on triaxial apparatus for the soils No.1 and No.2 were conducted with $6_{1} > 6_{1} = 6_{1}$ ($6_{6} = -1$) under two loading conditions at constant rates $\hat{\epsilon}_{1}$ or $\hat{\sigma}_{1}$ for each test. The rates for various tests have been changed over the range of up to 10^{5} times. Loading was performed until failure of the sample. The samples had been preliminary compressed under spherical stress tensor condition with a pressure of 5 kg/cm² and 7 kg/cm². The same apparatus have been used for long-term measurements (up to 500 days) of strain changes under constant stress state: $6_{1} = 6_{10} = 5$ kg/cm² or 7 kg/cm² with different values of 6_{1} .

The following symbols will be used:

The study on the effect of the time factor on deformation and strength of clay soils taking into account the action of all the three principal stresses has been conducted on the test arrangements I and II for the first time.

The tests on the arrangement I were conducted with 6=5 kg/cm² during the entire loading period, the loading being performed by increasing 6; for three values of the rates and with three different values of d_6 for each rate. The arrangement II has been used for time factor investigations under constant stress condition (6=5 kg/cm²; 6; = 5.2 kg/cm) and with a constant value of $d_6=-1$; 0; +1 for each test.

Shear strains \mathcal{E}_i and volumetric deformations θ were measured over the whole range of hardening under various conditions and also for ultimate strength state.

The studies on triaxial apparatus show of (plots on figs.5, 6, 7, 8) that the process of structure hardening (characterised

by shear and, especially, volumetric strains under the condition $\hat{\epsilon}_i = \text{const}$) appeared to be strongly dependant on the time given by the rate of strain (Similar results were obtained under conditions $\hat{\varsigma}_i = \text{const}$).

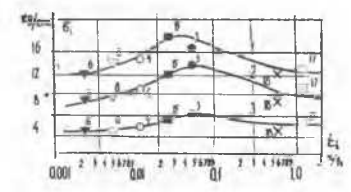


Fig. 5. Stress intensity 6; vs rate of strain intensity 5; , maintained constant for each test.

6= 6=5 kg/cm2.

Curve 1 corresponds to the ultimate strength state. Curves 2 and 3 correspond to values of & equal to 0.5% and 1.5% respectively. Numerals positioned at experimental points indicate test numbers.



Fig.6. Strain intensity ε_1 vs rate of strain intensity $\dot{\varepsilon}_i$ maintained constant for each test.

 $G_{\overline{u}} = G_{\overline{u}} = 5 \text{ kg/cm}^{\dagger}$. Curve I corresponds to ultimate strangth state.

Curve 2, 3 and 4 are plotted for values of 6; equal to 4 kg/cm², 8 kg/cm² and 12 kg/cm² respectively.

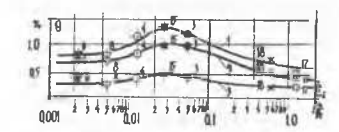


Fig. 7. Volumettic deformation Θ vs rate of strain intensity $\hat{\varepsilon}_i$ maintained constant for each test.

for each test. $61 = 6_{1} = 5 \text{ kg/cm}^2$. Curve 1 corresponds to ultimate strength state. Curves 2 and 3 are plotted for values of equal to 0.5% and 1.5% respectively.

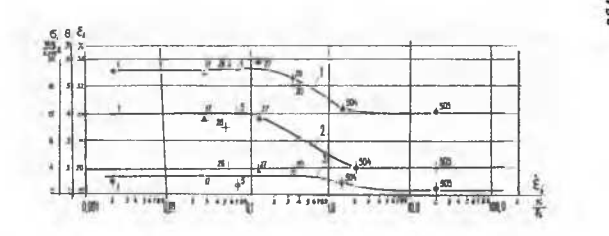


Fig. 8. Stress intensity σ_i (curve I), volumetric deformation θ (curve 2) and strain intensity ε_i (curve 3) vs rate of strain intensity ε_i having been field constant for each experiment. All curve correspond to ultimate strength state with $\sigma_{\mathbb{R}} = \sigma_{\mathbb{R}} = 7 \text{ kg/cm}^2$ Numerals above the experimental points correspond to test numbers.

The study time factor conducted on the arrangement I under the conditions $\dot{\sigma}_{\ell}$ =const with different values of d_{ϵ} confirmed the validity of results obtained on usual triaxial apparatus for $d_{\epsilon} = -1$.

As shows the analysis of experimental data the hardening depends on structural changes in soil during the loading. The characteristics of this hardening are represented by strains 9 and & which vary with time. Under different constant rate loading conditions time-dependent viscous resistances appear which effect θ and $\xi_{\rm t}$. The higher the loading rate, the gteater are viscous resistances, the shorter is the time until failure of the sample and the poorer is the hardening. At the same time, a total resistance grows along with a rate decrease until Gi achieves a value at which an optimum for hardening interaction of structural transformations and time-dependent viscous resistances begins. This process depends to a large extent on structural constitution, composition and condition of soil at the beginning of loading, as well as on loading conditions. For compact structural Permian clays reduction of loading rate causes 6 to go through a maximum after which 6; and 8 decrease, while ϵ_i slightly rises. Within the low rate region δ_i , ϵ_i and θ remain constant regardless further decrease in the rate. This decrease in 6 results from substantial reduction of viscosity forces and is a cause of corresponding decrease in Θ . Within the low rate region measured values of 6. represent the limit of long-term strength, while other values of 5; on the 6; we stimplot (fig.5) indicate long-term strength under given loading conditions. The observed features in the effect of the time factor on deformation and strength seem to be typical of compact clay soils for conditions studied /3/.

As shown by the evidence large values of $\mathfrak{S}^{\ell im}$ (Fig.5) correspond to high values of \mathfrak{S} (Fig.7), the latter being substantiable greater than volumetric strains \mathfrak{S} for long-term strength limit. Analysis of the soil hardening has shown that these high values of $\mathfrak{S}^{\ell im}$ are determined to a large extent by structural hardening, whereas timedependent viscous resistances do not exceed 50% of the difference between the maximum value of $\mathfrak{S}^{\ell im}$ and its minimum value which corresponds to the long-term strength limit.

If the soil, which has achieved a great degree of hardening, is subjected to prelimit long-term stresses G_i , G close to the ultimate ones, the limit of long-term strength is higher than the value obtained at very low loading rates. Therefore, the time factor acting under given constant-rate conditions brings about the hardening of soil.

Maximum values of 6_i , 0 and ϵ_i for disturbed loams are achieved in the low-rate region, where their variations are negligible (Fig. 8). Thus, for a given initial state of disturbed loam the limit of long-term strength is greater than all intermediate values of long-term strength. This fact is of practical importance in the construction of rolled earth fill structures.

The results of the time factor study will

be considered now taking into account the action of all three principal stresses. The data obtained from the tests with the sqil No.2 on the arrangement I with loading under conditions $\mathfrak{S}_i = \text{const}$ for different $d_{\mathfrak{S}}$ show that the longer time of deformation (determined by a given rate), the less is dilatancy of the medium (defined as deviator fraction of volumetric deformation Θ) and the weaker is its dependance on $d_{\mathfrak{S}}$ Fig.9.

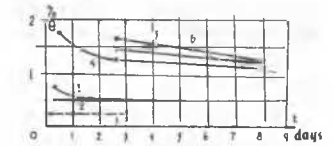


Fig.9.Component of volumetric deformation Θ created by the action of G_i under G_i = =const condition vs time t. Average stress G = 5.0

kg/cm² and stress intensity 6_i are held constant. 6_i is equal to 3.0 kg/cm² (curve 1; $6_i = -1$; 0 and +1), 5.0 $\frac{1}{2}$ curve 2: $6_i = -1$; curve 3: $6_i = +1$) and 8 kg/cm² (curve 4: $6_i = -1$; curve 5: $6_i = 0$; curve 6: $6_i = +1$).

As a result, the strength limit (Fig.10), volumetric strains and shape deformation appear to be independent of < 6 for the low 6 region.

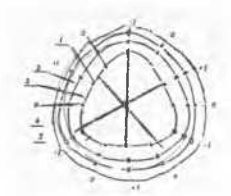


Fig. 10. Section through the ultimate state surface (in the space of principal stresses G_{Γ} , $G_{\overline{\Omega}}$, $G_{\overline{\Omega}}$) with a plane $G = 5 \text{ kg/cm}^2$ under condition $G_i = \text{const.}$ Radial rays are mark-

ed with corresponding values of α_6 . Curve 1 corresponds to the test with $\delta_i = 0.042$ kg/cm² per hour, curve 2 - with $\delta_i = 0.125$ kg/cm² per hour, curve 3 - with $\delta_i = 0.67$ kg/cm² per hour; circle 4 is plotted with the assumption of invariant condition of Mizes-Shleikher-Botkin with $\alpha_6 = -1$ and $\alpha_6 = 0.042$ kg/cm² per hour, circle 5 - with $\alpha_6 = -1$ and $\alpha_6 = 0.042$ kg/cm² per hour.

The decrease of the effect of doon ultimate strength (Fig.10) results in more simple expression for strength condition. For long-term strength limit with relatively low rates the latter may be assumed to depend only on two invariants 6 and 5 of stress state, whereas for rather high rates long-term three-dimensional strength is determined by the relation.

$$\phi(5, 5_i, \alpha_6, 5_i) = 0.$$
 (6)

It should be noted that the low loading rate region, where the effect of ϕ_6 becomes weaker, corresponds just to the actual rates of erection of the dam cores.

Observations of damping creep on the arrangement II conducted under a constant stress state confirmed the results of dilatancy and de studies performed on the arrangement.

1. As may be seen in Fig. 11, the dilatancy

of medium as well as the d_6 effect, observed initially for constant-stress loading ($6 = 5 \text{ kg/cm}^2$, $G_i = 5.2 \text{ kg/cm}^2$), appear to relax during long-term creep.

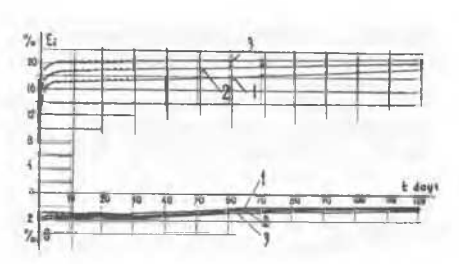


Fig.11.
Shape deformation and volumetric strain by time tunder acconstant stress

condition ($6 = 5 \text{ kg/cm}^2$ and $6 = 5.2 \text{ kg/cm}^2$) with different values of 6 = 6 equal to -1 (curves 1, 0 (curves 2) and +1 (curves 3).

The above features may be explained by the fact that with an increase of the loading time or duration of the action of a constant stress the strain anisotropy decreases due to creep or relaxation of soil.

The following general conclusion may be made from the above discussion.

Deformation, strength and dilatancy of soil, as well as the effect of the loading path on stress state are strongly dependent on the time factor resulting particularly in conventional nature of strength and deformation obtained for conventionally stabilized state of soil. The study on general features of strength and stress-strain state of clay soils should be conducted with compulsory consideration of the time factor under various loading conditions and different loading pathes. Interaction between the time factor stress tensor and the loading path rules out the application of the superposition principle in evaluating the effect of loading time on main features of deformation and strength.

III. This section was written by A.L.Kry-zhanovsky with the co-author E.I.Vorontsov. Deformation behavior of the sand soil cubical sample will be considered on the basis of the experimental data obtained with an apparatus / 4/3 which allows to predetermine different strains of the sample in three orthogonal directions and measurement of the corresponding stresses. A diagram of the experimental arrangement used and explanations of its structure are given in Fig.12.

At the first stage of deformation one and the same deformation was applied in all three directions until some value of volumetric deformation $\theta = \bar{\theta}$ which corresponded to a predetermined level of $\Theta(\omega)$; at the second atage the value of $\theta = \bar{\theta}$ has been maintained unchanged, while a value characterizing shape deformation of the sample ε_i was varied. In so doing, the rations between the principal strains were such as

to ensure a constant Lode-Nadai parameter α_{ϵ} in each test. Thus, at the second stage of deformation the pure shear deformation was obtained. Maximum rate of deformation was of 3.10⁻⁵ 1/hour and was selected so as to substantially eliminate the effect of the time factor on deformation behavior of sand soil. Measured stresses made it possible to handle the data in the invariant form. During the conduct of the experiments there were calculated 6 (level of isotropic stress) 6; (level of deviator of stress tensor) and α_{ϵ} (Lode-Nadai parameter of the type of three-dimensional stress condition), which corresponded to the respective values of θ ,

During the tests uniform medium grain sand was studied having different density (Fig. 13) which was achived by applying various methods of placing sand into the working chamber of the test apparatus (pouring through a funnel from a heqight of 5-7 cm, vibration with a needle vibrator to obtain greater density). Moisture content of sand corresponded to the airdry condition.

The test results were handled in coordinates 6 + 6; (Fig.13) and $\mathfrak{D}_{\kappa} + \varepsilon_{i}$, wherein $\mathfrak{D}_{k} = \frac{1}{3\sqrt{3}} \frac{6i}{6}$ (Fig.14).

Based on these results the following two questions will be discussed below: on stress condition of sand soil under the pure shear deformation and on the necessity of consideration of the interaction between the phases of saturated soils in determining of deformation properties.

The conditions of the pure shear deformation or those close to them occur in a large number of practical engineering problems, such as in the case of saturated soils under deformation without draining.

Phenomena of positive and negative dilatancy inherent to the majority of varieties of soils result in complicated path of development of stress condition corresponding to the pure shear deformation. These phenomena result in considerable difference of stress condition under the pure shear deformation of soil from stress condition under the pure shear of other materials, such as metals, where as is known the value of 6 should not change with an increase in ϵ_i . Plots given in Figs.13 and 14 directly show that the pure shear deformation is characterized by the following.

a) Value of $\mathfrak G$ depends upon the initial physical state of the sample and the level of preliminary isotropic compression, as well as upon the degree of development of shape deformation and type of strain condition (with different $\mathfrak G_{\mathfrak E}$). A change in $\mathfrak G$ occurs over the whole range of variation of $\mathfrak E_{\mathfrak E}$ studied. Depending on whether positive

or negative dilatancy phenomenon takes place, the value of 6 increases or decreases with

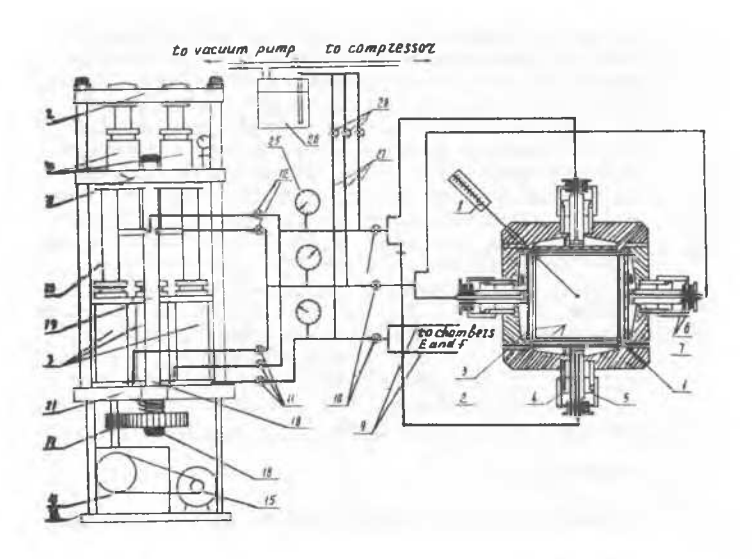


Fig.12. Diagram of the test bench.

1 -metallic wall; 2 -rubber membrane; 3 -perforated plate;

4 -movable rod; 5 -nut; 6 -bearing; 7 -gasket; 8 -device for measuring pore pressure; 9 -metallic tubes; 10, 11, 12, 28 -taps; 23, 14 - hydraulic cylinders; 15 -electric motor; 16 -gear box; 17 -tooth gear transmission; 18 -threaded coupling; 19 -vertical bar; 20 -intermediate movable plate; 21, 22 -lower and upper plates; 23 - columns; 24 -support frame; 25 - pressure gauge; 27 -compensation tank.

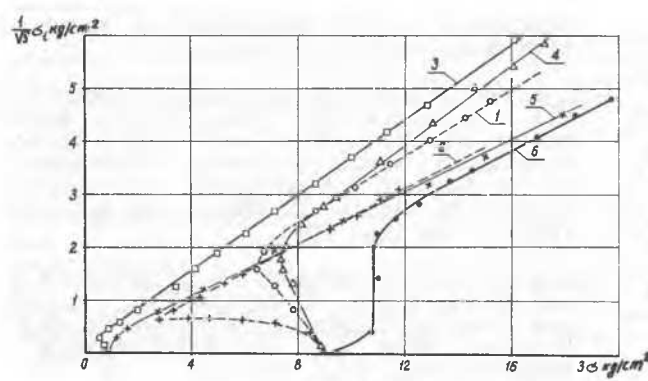


Fig. 13. Relationships $6_i = 6_i(6)$ based on the test results under pure shear conditions. $f = 1.44 \text{ g/cm}^3$; $1 - 6_{\odot} = 3 \text{kg/cm}^2$, $d_{\epsilon} = -1$; $2 - 6_{\odot} = 3 \text{ kg/cm}^2$, $d_{\epsilon} = +1$. $f = 1.64 \text{ g/cm}^3$; $3 - 6_{\odot} = 0.3 \text{ kg/cm}^2$, $d_{\epsilon} = -1$; $4 - 6_{\odot} = 3 \text{ kg/cm}^2$, $d_{\epsilon} = -1$; $5 - 6_{\odot} = 0.3 \text{ kg/cm}^2$, $d_{\epsilon} = +1$; $6 - 6_{\odot} = 3.0 \text{ kg/cm}^2$, $d_{\epsilon} = +1$.

Fig.14. Relationship & \(\simes \) & \((\text{D}_K) \)
Curves 1-6: the reference numerals are identical to those in Fig.13. Curves 7 and 8 were obtained based on the results of the tests with the pure deviatoric loading with \(\text{deg} = -1 \) and \(+1 \)
respectively

& growing, and the process may change its sign which indicates the possibility of transition of negative dilatancy into the positive one for one and the same soil as to its physical state depending on the degree of development of shape deformation.

b)Deformation hardening of the soil sample which has metastable structure results in monotonous increase in \mathcal{E}_i with \mathcal{E}_i growing. The intensity of growth of \mathcal{E}_i depends upon the same factors as those effecting a change in \mathcal{E}_i . It should be noted that deformation hardening is provoked not only by intensification of the internal friction forces, since in that case an increase in \mathcal{E}_i should

correspond to growth of 6. The experience shows that with 6; growing, 6 may either decrease or increase. Thus, the rearrangement of soil structure during the deformation exhibits as much effect on its hardening as the intensification of the internal friction forces. In particular, this implies that the expression of the characteristic of stress condition in the form of invariant \mathfrak{D}_K is not expedient in all cases of deformation as a variable in the relationship $\mathcal{E}_i = \mathcal{E}_i\left(\mathfrak{D}_K\right)$.

c)During the pure shear deformation a complicated loading path is performed in the space of the variables $6 \bullet 6$; The path

is defined by the initial physical state of the sample and the level of isotropic compression, as well as by the degree of the devolepment of shape deformation and type of three-dimensional stress condition. It should be emphasized that the analysis of the effect of loading path for sand soil in the above-mentioned coordinates was reported by a number of authors. Their experiments have revealed the absence of the effect of the loading path for a wide range of sands studied, this fact resulted in successful generalization of the data in the form of unambiguous relationship $\mathcal{E}_i = \mathcal{E}_i$ (D_K).Now, the results of the experiment of this report will be analysed.

Curve 7. 8 in Fig. 14 were obtained for a sample having one and the same initial physical state as in the case of curves 4 and 6, but not for the pure shear deformation which was replaced by the path of the pure deviatoric loading [2]. The comparison between the curves shows that they are substantially different, and therefore, that certain classes of loading paths in the space of 6 + 6 effect deformation properties of sand soil as well. This phenomenon may be explained by the fact that during the pure shear deformation the unloading and loading paths are combined coming one after another in the course of growth of ϵ_i . The paths corresponding to loading and unloading have the significance defined in [5]. The transition from the loading path to the unloading path under the pure shear deformation conditions is determined by physical state of a material, type of stress condition, equation of initial isotopic deformation and should be established by means of experiments. Therefore, it appears impossible to predict stress state under conditions of the pure shear of the sample on the basis of relationships obtained, for instance, with the pure deviatoric loading without additional information on deformation properties of a material during the unloading and on the transition from the unloading to the loading.

The role of the factor responsible for development of the pure shear deformation of completely saturated soil may be performed by practically uncompressible pore liquid (deformation without of liquid). Depending on whether positive or negative dilatancy is inherent to the soil under consideration, the role of pore liquid in its action upon the soil skeleton will by manifested with different sign. Deformation behavior of soil in this case will be determined by a sum of external stresses absorbed by the skeleton of soil element and volumetric stresses which appear as a result of the interaction between phases.

Relationship between total stresses and shape deformation of the sand soils studied in saturated state and during the tests without draining will correspond to plots 13 and 14.

It is not possible to devide the stress 6 into a fraction transmitted at the sample boundary and the volumetric stresses using. for instance, the results of the test of the skeleton according to the pure deviatoric loading scheme or with any other arbitrary path. In order to accomplish this it is necessary to conduct the test of the soil skeleton according to the pure shear deformation scheme. It should be emphasised that the active role of the interaction between the phases of a two-phase soil was revealed in principle, which brings about a wide variety of loading paths. Therefore, the concept of the independence of deformation properties of soil skeleton of the interaction between the phases was not experimentally confirmed.

REFERENCES.

- 1.Lomize G.M., Zakharov M.N. and Ivashenko I.N., USSR. Written contributions p.203. Proceedings of the Seventh International Conference on Soil Mechanics and Foundation Engineering, v.3, Mexico, 1969.
- 2.Lomize G.M., Kryzhanovsky A.L., Vorontsov E.I. and Goldin A.L. USSR. Study on deformation and strength of soils under three dimensional state of stress. Proceeding of the Seventh International Conference on Soil Mechanics and Foundation Engineering, v.1, Mexico, 1969.
- 3.Lomize G.M., Ivashenko I.N., Isakhanov E.A. and Zakharov M.N. On Deformation, Strength and Creep of Clayey Soils in the Cores of High-Head Dams. J. GIDROTEKHNICHESKOIE STROITELSTVO, 1970, No.11.
- 4.Kryzhanovsky A.L., Vorontsov E.I., Muzafarov A.A. Apparatus for Determination of Deformation Properties Strength of Soils, Inventor's Certificate No.302, 665 of February 12, 1971.
- 5. Iosilevich V.A., Didukh B.I. On Application of the Plastic Hardening Theory Reffered to the Definition of Soil Deformation, Collection of Works "VOPROSY MEKHAMIKI GRUNTOV I STROITELSTVA NA LESSOVYKH OSNOVANIAKH, Grozny, 1970.